E. Zimmerman and J. A. Pincock, *ibid.*, **95**, 2957 (1973); (c) *ibid.*, **94**, 6208 (1972). Several examples of mercury sensitized gas-phase photoreactions of 1,4-pentadienes, which afford [2.1.0]bicyclopentanes are known. See J. Meinwald and G. W. Smith, *ibid.*, **89**, 4923 (1967).
(11) H. Kristinsson and G. S. Hammond, *J. Am. Chem. Soc.*, **89**, 5970 (1967).
(12) (a) D. A. Plank and J. C. Floyd, *Tetrahedron Lett.*, 4811 (1971); (b) T. Matsuura and K. Ogura, *J. Am. Chem. Soc.*, **89**, 3846, 3850 (1967).
(13) K. B. Wiberg and D. E. Barth, *J. Am. Chem. Soc.*, **91**, 5124 (1969).
(14) E. Block, H. W. Orf, and R. E. K. Winter, *Tetrahedron*, **28**, 4483 (1972).
(15) J. A. Berson, W. Bauer, and M. M. Campbell, *J. Am. Chem. Soc.*, **92**, 7515 (1970).
(16) The fact that a single cyclopropane is formed from **7a** and **7b** contrasts with our earlier report that *cis*-cyclopropane formation may occur to a minor extent.[1b] It may now be stated with certainty that the cis epimer of **9** is not detectable among the reaction products, at least within the limits of our ^{1}H NMR analytical methods (0.5%).
(17) (a) H. E. Zimmerman and R. D. Little, *J. Am. Chem. Soc.*, **96**, 5143 (1974); (b) H. Kristinsson and G. W. Griffin, *ibid.*, **88**, 378 (1966).
(18) The triplet nature of the housane formation was not observed prior to our initial report of this work.[1b] Undoubtedly rearrangement of **8** to **7** during isolation occurred, and thus the former went undetected in our preliminary experiments (see Experimental Section).
(19) (a) H. E. Zimmerman and H. S. Swenton, *J. Am. Chem. Soc.*, **89**, 906 (1967); (b) *ibid.*, **86**, 1436 (1964); (c) M. H. Fisch and J. H. Richards, *ibid.*, **85**, 3029 (1963); (d) *ibid.*, **90**, 1547 (1968).
(20) 1,5-Bonding of the type proposed in path b is not without precedent. It has been established by labeling experiments that a 1,4-diacetylene studied by Zimmerman and Pincock [H. E. Zimmerman and J. A. Pincock, *J. Am. Chem. Soc.*, **95**, 3246 (1973)] reacts by a mechanism involving this type of initial bonding. Of course, conversely 2,4-bonding of the type proposed in path a is commonly advanced as the initial step in the di-π-methane rearrangement.[2]
(21) R. B. Woodward and R. Hoffmann, "The Conservation of Orbital Symmetry", Verlag Chemie, GmbH, Weinheim/Bergstr., Germany, 1970.
(22) It has been shown experimentally (ref 23a) and theoretically (ref 23b) that irradiation of samples in cylindrical cells in a merry-go-round apparatus may seriously affect the observed quantum yield when the sample cell contains a solvent of different refractive index from that employed in the antinometry cell, and similar criticisms might be advanced concerning our determinations with **7a** and **7b** despite the fact that the mini-go-round was employed with flat quartz cuvettes. In view of our ability to reproduce the reported quantum yield data for the photoisomerization of 1,1,3-triphenyl-3,3-dimethyl-1-propene, it appears that such arguments are invalid here, perhaps because of the essentially monochromatic light source used and the flat surfaces.
(23) (a) G. F. Vesley, *Mol. Photochem.*, **3**, 193 (1971); (b) M. D. Shetlar, *ibid.*, **5**, 287 (1973).

Reactions of Oxophlorines and Their π Radicals[1]

J.-H. Fuhrhop,*[2a] S. Besecke,[2a] J. Subramanian,[2a] Chr. Mengersen,[2a] and D. Riesner[2b]

Contribution from the Gesellschaft für Molekularbiologische Forschung, 3301 Stöckheim über Braunschweig, West Germany, and the Institut für Organische Chemie der Technischen Universität Braunschweig, 3300 Braunschweig, West Germany. *Received September 24, 1974*

Abstract: A detailed investigation of the reactivities of octaethyloxophlorine (**1**), its tautomer *meso*-oxyoctaethylporphyrin (**2**), and its metal complexes is presented. These compounds can be reversibly oxidized in a one-electron step. The oxidation potentials in neutral solutions are about 300 mV lower than those observed for related porphyrins. In alkaline solutions, an anion is formed by deprotonation, and these potentials are further lowered by 300 mV. Irradiation of the zinc complex with visible light first leads to a π radical. In the absence of oxygen, the π radical forms an ether linkage between the bridge oxygen and the methylene carbon of an ethyl group whereas, in the presence of oxygen, the radical is oxidized and decarbonylated, leading to the formation of an oxaporphyrin and carbon monoxide. A simple semiquantitative estimation of carbon monoxide using Dräger tubes is described. The macrocycle of the oxaporphyrin was converted by base to a biliverdin derivative. This reaction was fully reversed by acetic anhydride. The π radicals of oxophlorines dimerize in some organic solvents ($\Delta H_{293°} = -14$ kcal mol^{-1}), and the rate constant obtained by temperature-jump methods ($k_R = 2 \times 10^6\ M^{-1}$ sec^{-1}) is considerably smaller than that observed for unsubstituted porphyrin radicals. Further oxidation of **1** with Tl(III) salts leads to α,γ-dioxoporphodimethenes. Electrophilic substitutions in α-oxyporphyrins occur in the γ position. Some redox potential measurements on the amino and thio analogs of **1** are also presented, and a rationalization of the experimental data on the meso-substituted and unsubstituted porphyrin ligands aided by MO calculations is offered. The central conclusion drawn from experimental and model calculation is that meso hydroxylation of a porphyrin changes its benzene-type reactivity to that of a polyene.

Oxophlorines **1** and **3** and oxyporphyrins **2** and **4** constitute pairs of tautomers[3] which play an important part in the catabolism of heme[4] and are chemically different from unsubstituted porphyrins. Except for the formation of derivatives of the hydroxy group of **2** and the oxidative cleavage of iron complexes of **2**,[3,5-7] no further reactions of these systems have been investigated. We have found that oxophlorines and their metal complexes are oxidized at low potentials to π radicals which undergo a variety of interesting secondary reactions in high yields.

Results and Structural Assignments

π Radicals and Their Diamagnetic Dimers. Octaethyloxophlorine **1a** was oxidized by air, Fe(III) salts, and a variety of other agents to the π radical **6**. The magnetic susceptibility in chloroform was 1.6 μ_B. The neutrality of the radical follows from elemental analysis (no counterion) and chromatographic behavior. The electronic spectrum of **6a** consists of one band covering the whole visible range with a broad peak around 620 nm extending into the near infrared and a weak Soret band at 400 nm (Figure 1). Addition of acids to a chloroform solution of this radical leads to a diamagnetic cation of the nonoxidized oxophlorine **1a**, which shows a strong visible absorption at 680 nm.[3] In the infrared, both **1a** and **6a** produce strong bands around 1600 cm^{-1}, which indicates some double-bond character of the C=O bonds. The reaction **1a** → **6a** is fully reversible with reductants.

The radical **6a** seems to be always present in small amounts, even in spectroscopically pure preparations of **1a**, and hence one always finds an ESR signal[8-10] and no ^{1}H NMR[6,8-10] spectra. At low temperatures, however, the ESR signal disappears,[9] the electronic spectrum changes considerably, and well-defined, although broad, proton resonance signals are found.[9] A similar behavior has been observed for unsubstituted metalloporphyrin cation radicals[11]

Scheme I

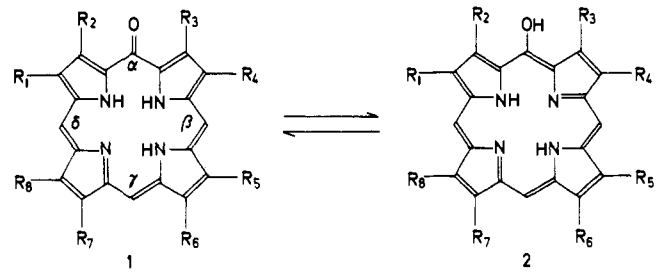

a $R_1-R_8=C_2H_5$
b $R_1, R_3, R_5, R_8=CH_3$; $R_2, R_4=C_2H_4$; $R_6, R_7=(CH_2)_2-COOH$
c according to 1b, but $R_2, R_4=C_2H_5$

Scheme II

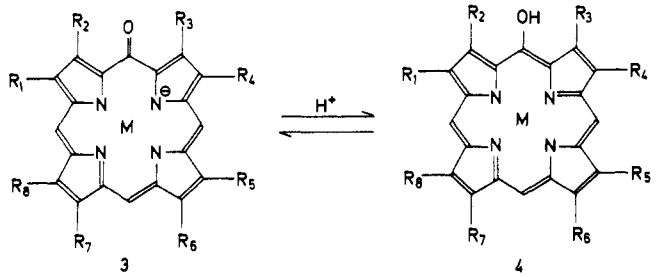

a M=2H
b M=Ni
c M=Zn

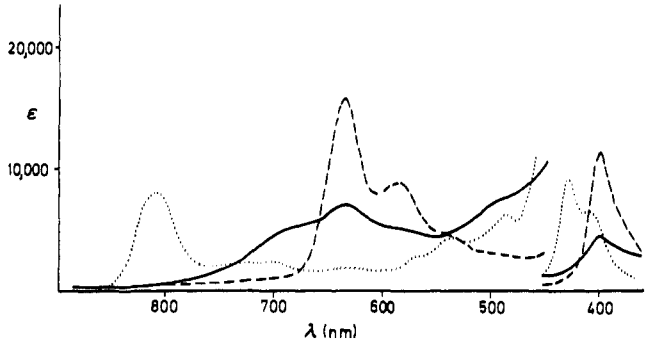

Figure 1. Electronic spectra of: (- - -) α-oxooctaethylphlorine (**1a**) in chloroform; (—) its π radical; and (• • •) the zinc complex of the radical (**6c**) in chloroform.

Scheme III

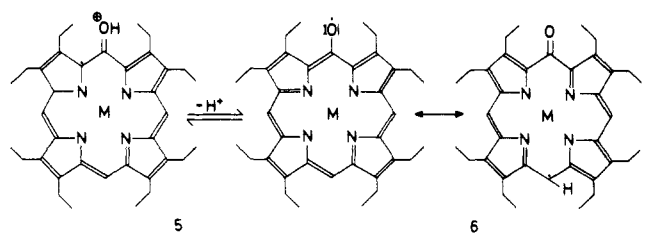

a M=2H
b M=Ni
c M=Zn

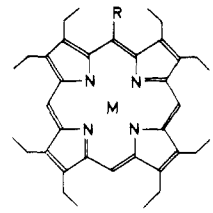

a R=H M=2H
b R=H M=Zn
c R=NH_2 M=2H
d R=NH_2 M=Zn
e R=SH M=2H
f R=SH M=Zn

Table I. Thermodynamic and Kinetic Data of the Dimerization of Oxophlorine Radicals and a Porphyrin Radical (at 20°C)

Compd	K,[a] M^{-1}	$-\Delta H$,[a] kcal mol^{-1}	$-\Delta S$,[a] cal deg^{-1} mol^{-1}	k_{12},[b] sec^{-1} M^{-1}
Oxophlorine radical **6a**	$(8 \pm 2) \times 10^3$	14 ± 1	32 ± 2	$(2 \pm 0.1) \times 10^6$
Nickel oxophlorine radical **6b**	$(6 \pm 2) \times 10^3$	15 ± 1	34 ± 2	$(2 \pm 0.2) \times 10^8$
Zinc porphyrin radical **7b** (from ref 11)	$(2.5 \pm 1) \times 10^4$	17.5 ± 0.4	38 ± 1	$(1.3 \pm 0.2) \times 10^8$

[a] From the temperature dependence of ESR spectra. [b] From temperature-jump method.

and was explained by a second-order reaction of a radical cation to form dimers with an enthalpy of $\Delta H = -17$ kcal/mol. We have repeated the identical set of experiments (temperature-jump kinetics, temperature dependence of ESR and electronic spectra, mass spectrum of solid material) on the radical **6a** and its nickel complex **6b** and found similar behavior as observed with the zinc octaethylporphyrin radical dimer. The presence of a dimerization process has been established in both cases since the dependence of the relaxation times upon concentrations corresponded to a second-order reaction (see Figure 7). It is noteworthy that the metal oxophlorine radical **6b** and the meso-unsubstituted radical of zinc porphyrin **7b** recombine with similar, nearly diffusion-controlled rates. The free radical from the metal oxophlorine, however, dimerizes slower by a factor of about 100 (see Table I) than the radical from the free ligand. At higher concentrations of the nickel oxophlorine radical, there are indications that another reaction step is involved in the dimerization process (see Experimental Section), which has not been clarified so far. The nickel oxophlorine radical dimer also produces a broad charge transfer band with a maximum close to 900 nm and its enthalpy of formation is comparable to that of the radical of **7b**. Therefore, the same arguments which have been put forth for the $(ZnOEP)_2^{2+}$ π-π' dimer also hold good for the oxophlorines and need not be discussed in greater detail.

In the infrared, the unoxidized *meso*-oxyporphyrins **4b** and **4c** do not absorb around 1600 cm^{-1}, whereas both radicals **6b** and **6c** do. This again is in favor of the formulation of the neutral oxophlorine complexes **6** rather than the protonated cations **5**, in the case of the radicals. Elemental analysis and chromatographic behavior again confirmed this point.

Electrochemistry. Voltammetric and polarographic measurements (Table II) have yielded low oxidation potentials for the oxy- and aminoporphyrins (e.g., **7c,d**), but higher potentials for the thio derivatives which are comparable to those of meso unsubstituted porphyrins (e.g., **7e,f**). The reduction potentials show similar trends; the oxy and amino derivatives are reduced more easily than the thio- or unsubstituted porphyrins. The electrochemical behavior of free oxooctaethylphlorine **1a** is complicated, and only a portion of the results will be reported here.

In both butyronitrile and dichloromethane, oxooctaethylphlorine **1a** yields similar cyclic voltammograms (Figure

Table II. Polarographic Midpoint Potentials for Substituted Porphyrins and Their Metal Complexes[a-c]

System	Oxidation $E_{1/2}(1)$	Reduction $E_{1/2}(1)$	Reduction $E_{1/2}(2)$
α-Amino-OEP	0.34 (0.064 ± 0.003)	−1.43 (0.052 ± 0.008)	−1.74 (0.041 ± 0.008)
Oxy-OEP	0.35[d] (0.063 ± 0.008)		
Zn(oxa-OEP)	0.34 (0.059 ± 0.002)	−1.00 (0.060 ± 0.004)	
α-Mercapto-OEP	0.79 (0.048 ± 0.005)	−1.69 (0.050 ± 0.003)	
Zn(α-amino-OEP)	0.20 (0.070 ± 0.006)	−1.69 (0.064 ± 0.005)	
Zn(α-mercapto-OEP)	0.52 (0.045 ± 0.005)	−1.17 (0.056 ± 0.002)	
Zn(oxy-OEP)	0.20 (0.058 ± 0.005)	−1.67 (0.057 ± 0.010)	
Zn(α,γ-dioxo-OEP)	0.83 (0.057 ± 0.004)	−0.54 (0.056 ± 0.003)	−0.72 (0.064 ± 0.003)
Zn(oxameso-porphyrin)	0.35 (0.056 ± 0.001)	−0.96 (0.063 ± 0.003)	
Ni(Oxo-OEP)	0.45 (0.065 ± 0.001)		
Ni(α-hydroxy, γ-cyano-OEP)	0.84 (0.058 ± 0.010)	−0.93 (0.047 ± 0.004)	

[a] OEP stands for octaethylporphyrin. [b] Oxidation potentials were measured with a rotating platinum electrode in butyronitrile as solvent. Reduction potentials were measured with a dropping mercury electrode in Me_2SO as solvent. [c] The estimated error in the half-wave potentials is ±0.01 V. The magnitude of $(E_{3/4} - E_{1/4})$ in volts is given in parentheses for each measurement. [d] An additional wave appears at −0.05 V which increases in height on repeated scanning of the polarogram (see text).

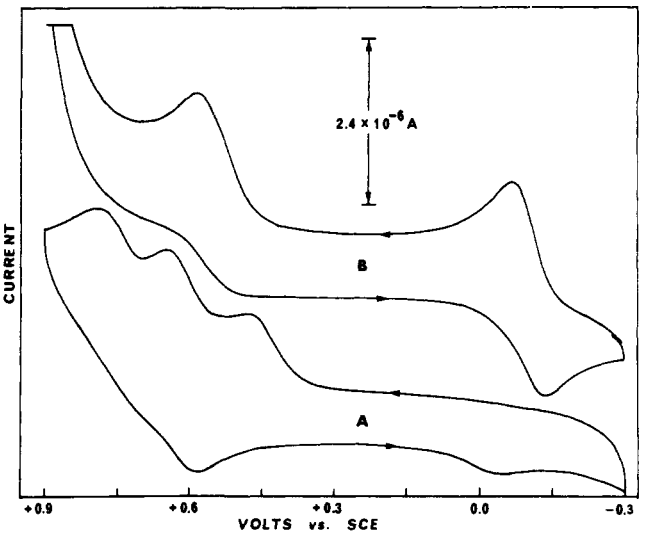

Figure 2. Cyclic voltammogram of oxyoctaethylporphyrin (~10^{-4} *M*) in dichloromethane containing 0.1 *M* tetra-*n*-butylammonium perchlorate, sweep rate 0.04 V/sec: (A) without base; (B) the medium contains a few drops of saturated solution of potassium *tert*-butylate in *tert*-butyl alcohol.

Scheme IV

neutral solutions

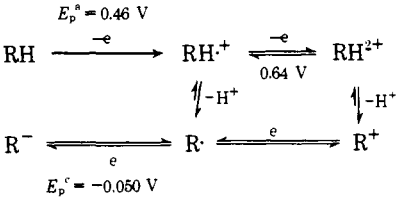

basic solution

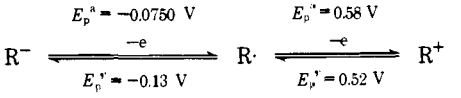

2A). The first oxidation peak occurs at $E_{p_1}^a$ = 0.46 V vs. SCE in CH_2Cl_2. This step is not reversible. But it is likely to be a one-electron oxidation as indicated by dc polarography ($E_{3/4} - E_{1/4}$ = 0.068 V, see Table II). Also since the spectral data confirm the formation of a radical from the oxidation of **1a**, we tentatively assign this step to the reaction RH → RH·⁺, where RH is oxophlorine **1b**. A second oxidation step occurs at $E_{p_2}^a$ = 0.64 V in CH_2Cl_2 which is reversible. A third oxidation step occurs at $E_{p_4}^a$ = 0.78 V, but this will not be considered further. In the reverse sweep, a reduction peak appears around $E_{p_3}^c$ = −0.07 V vs. SCE. The height of this peak increases with repeated scannings of the voltammogram. The same behavior is also noticed in dc polarography. A small wave appears around $E_{1/2}$ = −0.05 V in butyronitrile which increases in height after prolonged scanning of the polarogram. In dichloromethane solutions of **1a** containing excess of a base-like potassium *tert*-butylate, a well-defined reversible oxidation step occurs with $E_{p_3}^a$ = −0.07 V vs. SCE ($E_p^a - E_p^c$ = 0.06 V) (see Figure 2B). The peak at $E_{p_1}^a$ = 0.46 V is absent, but the second oxidation step occurs at $E_{p_2}^a$ = 0.70 V which is also reversible ($E_p^a - E_p^c$ = 0.06 V). The above observation can be explained as follows. Oxophlorine **1a** contains three ionizable protons, and it appears at least one of the protons easily dissociates to form a neutral radical which is reduced at a more negative potential to give rise to the reduction peak around −0.07 V in dichloromethane solutions. This is clearly established by the voltammogram obtained in basic solutions in which the neutral radical is directly formed from the anion of **1a** (see Figure 2B). We propose the mechanism shown in Scheme IV for the oxidation of oxophlorine in neutral and basic solutions. The second oxidation step occurs at nearly the same potential in both neutral and basic media. Hence it is likely that the ionization of a proton occurs in the first oxidation step of **1a**, leading to the irreversibility of the first step in neutral solutions. This view is also supported by elemental analysis and chromatographic behavior. The behavior of the zinc complex of **1a** is qualitatively similar to that of the free ligand. Irreversible steps are observed in neutral solutions in dichloromethane. The cyclic voltammogram of the Zn complex is not similar to that of the free ligand **1a** in neutral solutions but, on the addition of base, a well-defined reversible oxidation step is observed at low potential which is quite similar to that obtained for the free ligand. The behavior of the zinc complex in basic solutions also strengthens the validity of the mechanism proposed above. The voltammetric data are summarized in Table III. A more detailed electrochemical study is in progress.

Photochemistry. When a chloroform solution of oxooctaethylphlorine **1a** was chromatographed on alumina in the presence of air, the radical **6a** was formed, which could be isolated in almost quantitative yield and was identified by ESR spectra, electronic spectra, and susceptibility measurements. If **6a** was left on the column or in chloroform solution for longer periods of time, then the α,γ-dioxoporphomethene **8a** was formed in 60% yield. The analogous reaction occurred when the zinc complex **4c** or **6c** was irradiated in the presence of air in polar solvents, e.g., pyridine. No product other than **8b** could be identified in the reaction, which is reminescent to the oxygenation of phenol or aniline

Table III. Cyclic Voltammetric Data for Some Porphyrin Systems in Dichloromethane at 295 K[a,b]

System	E_p^a, V	E_p^c, V	Remarks
Oxy-OEP (1a)	I 0.46	−0.07	Irreversible
	II 0.64	0.57	Reversible
	III 0.78		
Oxy-OEP (1a)	I −0.07	−0.13	Reversible
(with base)[c]	II 0.58	0.52	Reversible
Zn(oxy-OEP)	I 0.32	0.17	Irreversible
	II 0.50	0.25	Irreversible
Zn(oxy-OEP)	I −0.22	−0.29	Reversible
(with base)[c]	II 0.31	0.21	Irreversible
α-Mercapto-OEP	I 0.94	0.87	Reversible
Zn(α-mercapto-OEP)	I 0.79	0.73	Reversible
α-Amino-OEP	I 0.35	0.28	Reversible
Zn(oxa-OEP)	I 0.48	0.41	Reversible
Mg(OEP)	I 0.58	0.51	Reversible

[a] The solvent is dichloromethane containing 0.1 *M* tetra-*n*-butylammonium perchlorate. The concentrations of the porphyrin compounds were in the range 10^{-3}–10^{-4} *M*. [b] The sweep rate was varied between 0.16 and 0.01 V/sec. The peak potentials vs. SCE are independent of the sweep rate in this range. The estimated error in the potentials is ±0.01 V. Values of Mg(OEP) are given for comparison. [c] A few drops of a strong solution of potassium *tert*-butylate in *tert*-butyl alcohol were added to the dichloromethane solutions.

resulting in *p*-benzoquinone. The most interesting reaction of oxophlorine accelerated by the action of light was the air oxidation of the zinc complex **4c** in apolar solvents e.g., a mixture of benzene and methylene chloride. Under these conditions, the only isolable product (yield 15–20%) was the oxaporphyrin **9b,** which decomposed rapidly under the reaction conditions to unidentified compounds with optical absorptions below 550 nm. Hence **4c** was irradiated only shortly (ca. 15 min) to achieve about 30% transformation so that ca. 70% of the starting material and 15–20% of **9b** could be obtained. The other product of this reaction was carbon monoxide, which was identified and estimated semiquantitatively by a simple standardization procedure using Dräger tubes. If **4c** was photooxygenized completely, not taking care of the further decomposition of the oxaporphyrin **9b,** then 80–90% of the theoretical amount of carbon monoxide could be reproducibly detected, assuming that one molecule of CO was formed from one molecule of **4c.** In a control experiment, it was shown that irradiation of **9b** did not yield carbon monoxide. Therefore it seems quite obvious that the keto group of **4c** is lost in the course of this reaction as carbon monoxide and that, in the reaction with molecular oxygen, one atom of oxygen is introduced into the tetrapyrrole skeleton.

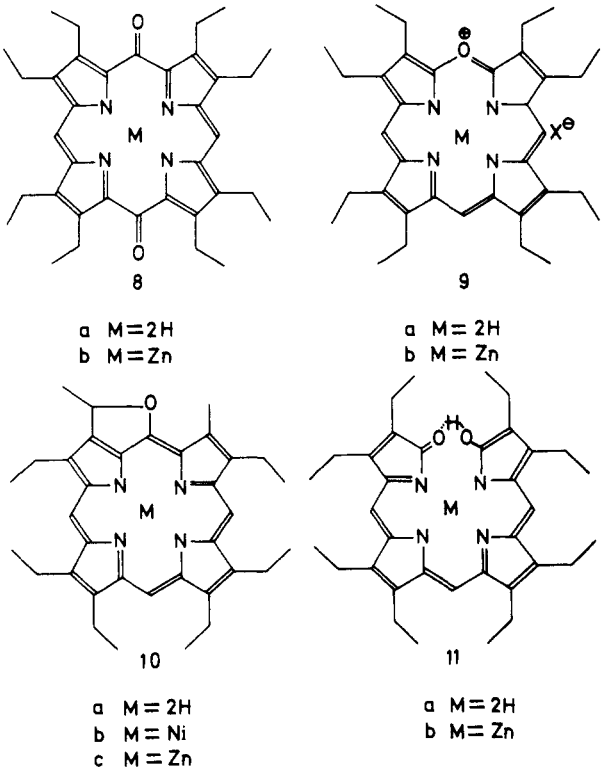

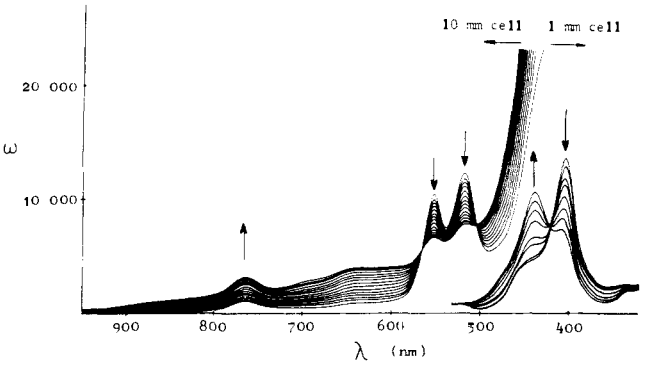

Figure 3. Spectrophotometric changes during the photooxidation of nickel oxyporphyrin **4b** to its π radical **6b.**

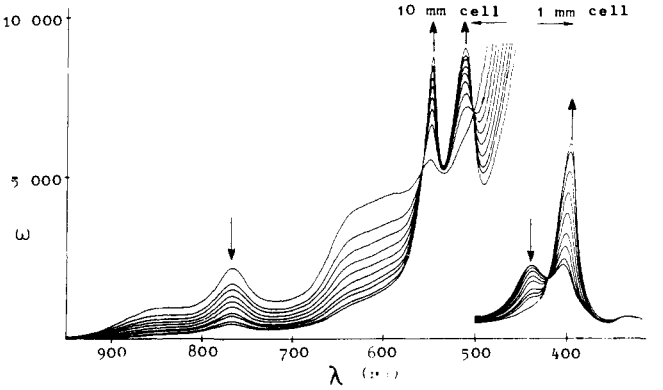

Figure 4. Spectrophotometric changes during the photocyclization of nickel oxyporphyrin radical **6b** to the oxole **10b.**

The reaction of nickel oxophlorine **4b** was different from that of the zinc complex; the primary photoproduct was also π radical **6b** as judged by ESR and electronic (Figure 3) spectra, but this was not further oxidized on prolonged irradiation. It rather cyclized intramolecularly and irreversibly in high yield (66%) to the oxole porphyrin **10a,** which led to the reappearance of a porphyrin-electronic spectrum (Figure 4) (^{1}H NMR δ 6.56 (quartet, 1 H at 2′), 2.20 (doublet, 3 H at 2″); 9.55, 9.52, and 9.43 (three singlets, methine H, β, γ, δ)). An oxaporphyrin or a dioxoporphodimethene could not be detected in appreciable yields. The π radicals **4b** and **4c** could be converted to the cyclic ether compounds **10a** and **10b** in 60% yield, when irradiation was performed under pure nitrogen. **10a** and **10c** rapidly decomposed to unidentified porphyrins with light and oxygen, but the nickel complex was stable.

Oxaporphyrins. Oxaporphyrins have been obtained earlier in the form of iron complexes by the oxidation of hemin in the Warburg procedure, using oxygen and ascorbic acid in pyridine.[3] In the reported electronic spectra of these compounds,[3] the intensity of the band in the ultraviolet is nearly double that of the visible band, which probably points to some porphyrin impurity. The purified zinc complex **9b** shows a relatively stronger visible band (Figure 5). The ^{1}H NMR spectrum contains two types of methine proton sig-

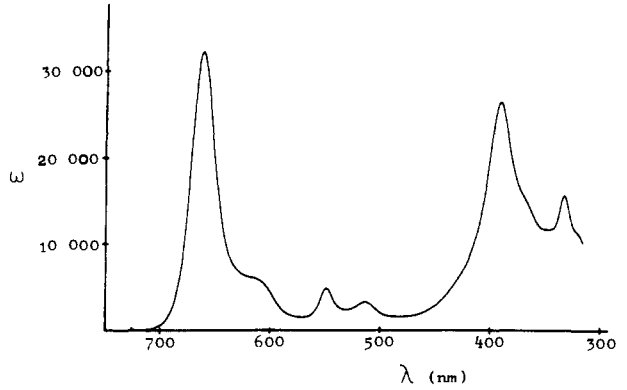

Figure 5. Electronic spectrum of zinc oxaoctaethylporphyrin **9b** in chloroform.

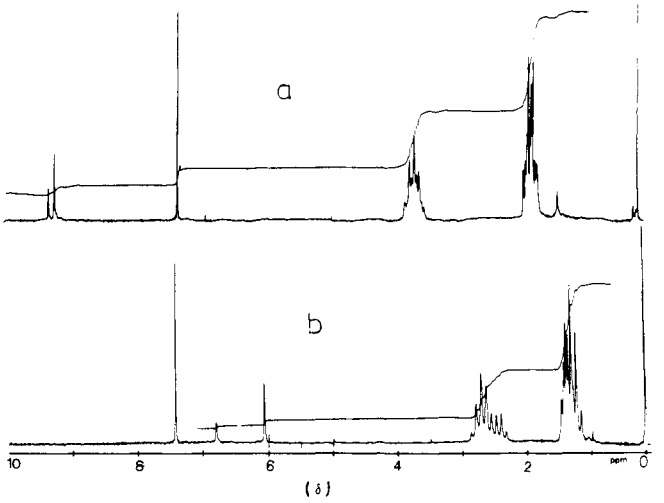

Figure 6. (a) ^{1}H NMR spectrum of zinc oxaporphyrin **9b**. The low-field methine proton signals indicate a large ring current effect. (b) ^{1}H NMR spectrum of octaethylbiliverdin **11a**.

nals, and the chemical shifts indicate that both the protons are highly deshielded (Figure 6a). Oxaporphyrins yield well-defined mass spectra which contain strong molecular ion peaks in sharp contrast to the metal biliverdinates (e.g., **11b**), for which usually no mass spectra could be obtained under ordinary conditions.[12]

On addition of small amounts of base, the macrocycle of oxaporphyrin **9b** is rapidly and quantitatively opened up to form the zinc biliverdinate **11b** which did not yield a well-resolved NMR spectrum. When, however, the zinc was removed by the action of acids, a good spectrum of octaethylbiliverdin **11a** could be obtained, in which the methine proton resonance occurs at much higher magnetic field (Figure 6b) than those observed for oxaporphyrin. The opening of the oxaporphyrin macrocycle could also be effected by acids (e.g., HCl), but here a larger excess of acid is necessary and simultaneous demetalation is usually observed, which is always followed by some irreversible decomposition of biliverdin chromophore. The oxaporphyrin **9b** could be regenerated in almost quantitative yield by heating a solution of **11c** in acetic anhydride and using a work-up procedure which does not involve acidic or basic conditions.

The redox potentials of **9b** (Table II) indicate that it can be reduced and oxidized more easily than the related zinc porphyrin **7b** and is of comparable reactivity to the zinc oxyporphyrin **4c**. This observation explains the instability of **9b** under the conditions of photoreaction in which it is formed from **4c**.

***meso*-Dioxoporphomethenes ("Porphoquinones") and α-Oxy-γ-formylporphyrin Derivatives.** When the oxophlorine **1a** was prepared by the oxidation of ZnOEP **7a** with thallium trifluoroacetate following Smith,[13] we always observed two by-products in varying yields. One was the zinc complex **8b** of α,γ-dioxoporphodimethene (**8a**), which had been prepared earlier from zinc α-amino-OEP **7c**.[14] It is now more easily available in almost quantitative yield by the photooxygenation of **6c** in pyridine.

8b separates into two fractions A and B when chromatographed on silica gel. Both fractions have identical electronic spectra in dilute chloroform solution (λ_{max} 576 nm), but, in concentrated solution, the compound B, which runs slower on the chromatogram, turns green (λ_{max} 620 nm). The compound A with the large R_f value stays always red in solution. B is reversibly reduced by sodium dithionite in chloroform solution to a rather stable π radical with a narrow ESR signal (g = 2.0040, line width 2 G). A on the other hand rapidly and irreversibly decomposes to unidentified compounds, and only weak unstable ESR signals were observed. Mass and infrared spectra as well as elemental analysis of both compounds are close to being identical and are in agreement with the proposed structure of **8b**. The reduction potentials are −0.54 V vs. SCE for both A and B. Various interpretations have been considered for these findings. Crystal structure work on the green compound B suggests that it may be a dimer even in solution which is stabilized by interactions with protic solvents.[32] Much more experimental work, however, is required to substantiate this hypothesis and the conclusions derived from it.

From the oxidation of zinc octaethylporphyrin by thallium trifluoroacetate, we also isolated a violet compound (λ_{max} 539 nm) as a second by-product (yield 5%) which, according to the mass spectrum, elemental analysis, and infrared and electronic spectra, was identified as the α,β-dioxoporphomethene **12a**. The ^{1}H NMR spectrum consists of two different deuterium exchangeable NH (or OH) proton signals (δ 9.96 and 8.69 ppm) which would correspond to structure **12a**, but it also shows two different methine proton signals (δ 6.62 and 4.66 ppm), which does not agree with our proposal. From the ^{1}H NMR spectrum and elemental analysis, we propose the hydrate structure **12b**. **12** does not form metal complexes, probably because of the low acidity of the NH proton in the isolated pyrrole unit, and it is reduced to the oxophlorine **1a** in 60% yield by the action of sodium borohydride. If one takes into account the "aromatic" character of the porphyrin macrocycle, the easy reducibility of the α,γ-dioxoporphomethenes, the stability of some of the resulting radicals, and the formal similarity of these diketones with quinones, then systems like **8** could be called "paraporphoquinones", which is chemically more perceptual than the systematic name. α,β-Dioxoporphomethenes would then be "orthoporphoquinones".

One of the most successful electrophilic substitution reactions in the porphyrin field and often the only way to introduce new carbon substituents is the Vilsmeier formylation procedure,[15] which we applied to the nickel oxophlorine **4b**. The formylated oxyporphyrin **13a** was the main product (yield ca. 70%), probably with some admixture of the β,γ-diformyl product (~10%). **13a** was converted by standard methods to the cyanoacetoxy derivative **13c**.

Discussion

In this section, the reactivity of the oxophlorines will be correlated to their spectroscopic behavior and electronic structure. The central aim will be to show and to rationalize how and why the hydroxylation of one methine bridge of the porphyrin macrocycle profoundly changes the properties of the whole π-conjugation system.

Table IV. SCF Energies for Porphyrin, Oxophlorine, and Oxaporphyrin Free Bases (Calculated by PPP Method)[a]

	Highest bonding orbital (in eV)	Lowest antibonding orbital (in eV)
Porphyrin	−8.322	−4.054
Oxophlorine	−8.141	−4.315
Oxaporphyrin	−8.886	−4.710

[a] The SCF parameters are:[20] $U_C = -11.16$, $U_N = -14.12$, $U_N = -24.56$, $U_O(C=O) = -17.7$, $U_{O+} = -33$, $\beta_{CN(pyrrole)} = -1.80$, $\beta_{CN(pyridine)} = -2.75$, $\beta_{CO+} = -2.8$, $\beta_{CO} = -1.2$ eV.

Table V. Electronic Transition Energies (Singlet–Singlet) and Oscillator Strengths in Oxophlorine and Metal Oxaporphyrin (Calculations by PPP–SCF–CI Method[a,b])

	Transition energy, eV		Osc strength	
Compd	Calcd	Exptl[c]	Calcd	Exptl[c]
Oxophlorine 1a	1.84	1.95	0.43	0.08
	2.28	2.11	0.10	0.07
	3.44	3.10	2.60	1.40
Oxaporphyrin	1.80	1.87	0.39	0.10
Metal complex	3.00	3.14	0.07	0.50
E.G., 9b	3.56		3.00	
	3.75	3.70	0.23	0.15

[a] See Table IV for the SCF parameters. For the oxaporphyrin, $U_N = -20.04$ eV for all the four nitrogen atoms was chosen. [b] Twenty configurations were considered for CI. [c] Experimental data from the present work.

Table VI. Spin Densities and Proton Hyperfine Couplings in the Oxophlorine Radical 6a (Calculated by Hückel–McLachlan Method)[a]

		a_H, G	
Position[b]	ζ^π (calcd)	Calcd[c]	Exptl
α	0.061		
β	0.196	−4.6	4.6
γ	0.256	−5.9	4.6
δ	0.196	−4.6	4.6

[a] Hückel parameters used were $h_N = 1.0$, $h_O = 1.4$, $\beta_{CN} = 1.0$, $\beta_{CO} = 1.2$. [b] See structure 1 for the numbering of positions. [c] Proton hyperfine couplings were calculated using the relation $a_H = -23\zeta_C\pi$.

From the electronic, infrared and ^{1}H NMR spectra, it can be concluded that carbon (CH_3, CHO, CN) and sulfide (SH) substituents on the methine bridges are always single bonded, and the tetrapyrrolic chromophore behaves always similar to an unsubstituted porphyrin (class I substituents). On the other hand, *meso*-hydroxy or -amino functions (class II substituents) are either present as such or as keto (imino) groups, depending on the oxidation state of the porphyrin ligand, pH, solvent, etc. It is so noticed, that the class I substituents have only relatively little influence on the redox reactivity of the porphyrin, whereas class II substituents facilitate reversible and irreversible oxidations (and reductions) of the tetrapyrrolic system. Qualitatively one might state that type II substituents shift the behavior of the porphyrin macrocycle from the aromatic to the polyene type. It can also be said that the methine bridge opposite to a class II substituent is especially vulnerable to electrophilic and nucleophilic attack. This behavior is also found in phlorines, where a hydrogenated methylene bridge is present. Replacement of a proton on a class II substituent, e.g., by an acetyl group, usually converts it to class I.

The results of Pariser-Parr-Pople (PPP) SCF calculations[16] on oxyporphyrin and oxophlorine indicate that the energy difference between a_{1u} and a_{2u} bonding orbitals is larger for the oxophlorine structure. The highest bonding

Scheme V

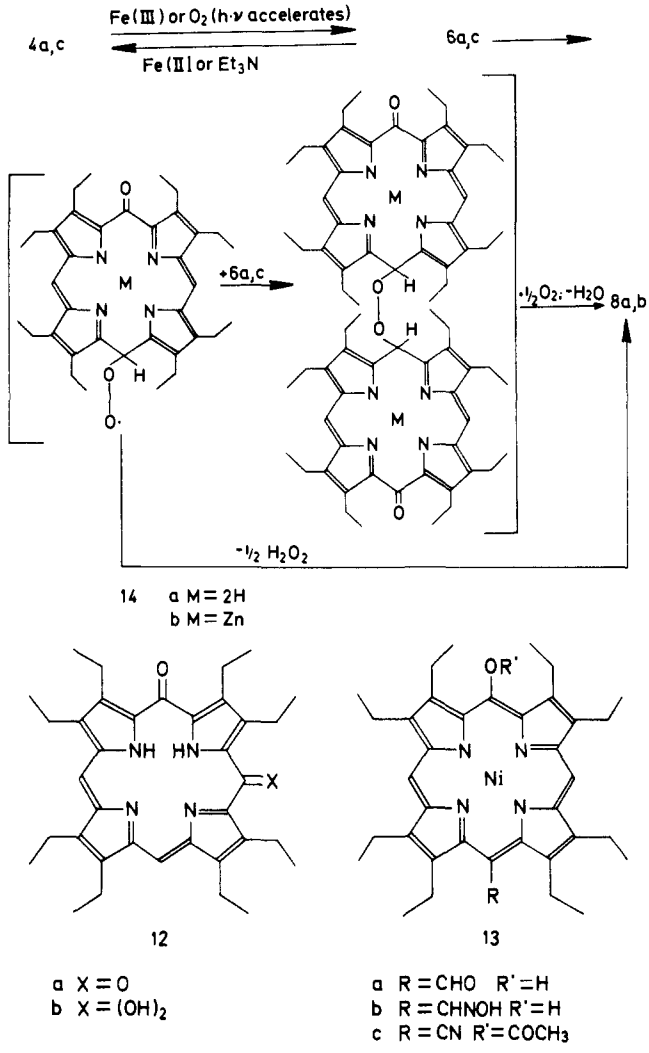

level in oxophlorine is about 0.200 eV higher than that in a porphyrin (see Table IV). Thus qualitatively theory rightly predicts that oxophlorine is more easily oxidizable than a porphyrin. However, the difference in the experimental $E_{1/2}$ values of oxophlorine and porphyrin is larger (0.350 V) than the predicted value of 0.200 V. Furthermore, PPP-SCF calculations including configuration interaction[17] predict the electronic spectra of oxophlorine within reasonable accuracy (Table V).

Hückel-McLachlan calculations[18] were performed to understand the spin density distribution in the oxophlorine radical so as to interpret the ESR spectra and also the reactivity of the radical. The hyperfine coupling constants are reasonably predicted as seen in Table VI, indicating the reliability of the wave function for the ground state of the radical. The large spin density at the methine bridge opposite to the carbonyl group indicates that the electrophilic attack will preferentially take place in the γ position. This is in agreement with early interpretations of phlorine reactivity.[19,20] The calculated π-bond order of C-O group in this radical is 0.700. This is in good agreement with electronic spectra (phlorine-type spectrum) and ir data.

Depending on the central metal ion, solvent, and the presence or absence of air and/or light, three main types of reactions of octaethyloxyporphyrins are encountered. (1) Chemical oxidation of nickel and zinc complexes in any solvent or photochemical oxidation in pyridine leads to α,γ-dioxoporphomethenes **8** (Scheme V). (2) Irradiation of a zinc oxophlorine in nonpolar solvents in the presence of air

Scheme VI. Possible Pathways from Oxophlorines to Biliverdins[a]

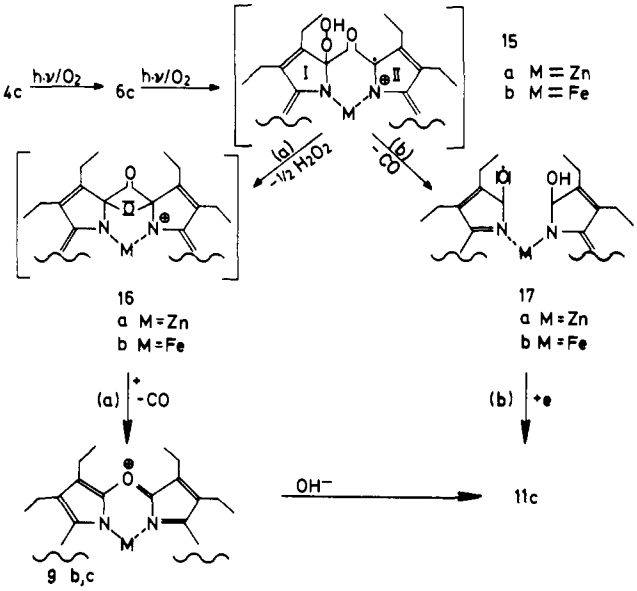

[a] (Path a) Sequence with an oxaporphyrin as only isolable primary product. This is found in in vitro reactions, such as photooxygenation of zinc oxophlorines and the coupled oxidation of iron oxophlorines. (Path b) Intramolecular migration of OH radical leading directly to a ring opened biliverdin derivative. This pathway might be followed in the natural degradation of protein bound heme, where it has been shown that both terminal oxygens in bile pigments come from molecular oxygen.

produces an oxaporphyrin **9b** and carbon monoxide. Presumably a similar reaction proceeds in the biological oxidation of heme, wherein, however, only biliverdin has been found so far. In the in vitro oxidation of heme by systems producing hydrogen peroxide, liberation of carbon monoxide has not yet been detected. Scheme VI gives a short account of the possible courses of these reactions. (3) Irradiation of the zinc complex with visible light under anaerobic conditions leads to cyclization involving the exocyclic oxygen and the benzylic carbon of an adjacent ethyl group. This reaction also occurs in the presence of oxygen when nickel is the central ion (Scheme VII).

All the reaction pathways 5-7 start with the π radicals **6** rather than the unoxidized oxyporphyrins **4**. Reaction 1 can be rationalized as the reaction of the radical **6** in the dark with triplet oxygen, which is accelerated, when the porphyrin is in an excited state (Scheme V).

In the second reaction, an oxygen molecule is added to an α-pyrrolic carbon atom adjacent to the excited C=O bond, where an unpaired electron is localized on the oxygen. The indicated rearrangements then take place spontaneously, possibly driven by the steric strain which is forced onto the porphyrin macrocycle, when an α-pyrrolic carbon atom has a tetrahedral configuration. In fact, such adducts have never been isolated from porphyrins; they always break apart to form ring-opened bilatrienes. A reaction similar to the one of the Scheme VI also occurs with unsubstituted metalloporphyrins, where the methine carbon is not split off as carbon monoxide but is rather retained as formyl group in the resulting formyl biliverdins.[21] The primary intermediate in the latter reaction is presumably a dioxetane **20,** which rearranges in the indicated way. The four-membered ring, in the case of oxophlorine, should be unstable because of large electron repulsion and steric hindrance in such a three-oxygen system. Hence we propose Scheme V; here it is easy to envisage the removal of an OH fragment from the radical **15** (path a). The hydroxyl group of **15** could, however, also migrate directly to the adjacent pyrrolic site in

Scheme VII

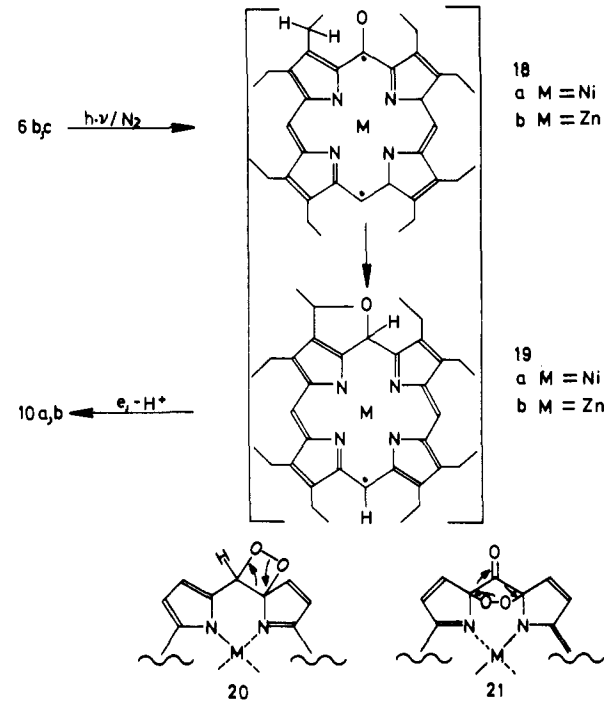

the ring II (path b). Subsequent opening of the macrocyclic ring and simultaneous elimination of carbon monoxide could lead directly to a biliverdin. Such reaction is not observed in the in vitro experiments but might occur in the natural degradation of heme, where no hydrolysis reaction is involved in the formation of biliverdin.[4a] Another possible intermediate in the biological pathway is the dioxolone-type adduct **21,** which has been proposed by Kenner et al.[4b] As long as none of the dioxygen adducts **15** or **21** can be trapped and studied in detail, a clear-cut experiment to distinguish between the two pathways seems impossible. The formulation of **21,** however, complicates the scene somewhat, because it implies that the reactions of oxophlorines in vitro and in vivo are basically different. We are unable to envisage any plausible reaction sequence, which leads from **21** to an oxaporphyrin like **9b.** On the other hand, from the radical peroxides like **15,** both oxaporphyrin and biliverdin derivatives should be easily formed, as is indicated in Scheme V.

Reaction 3 would correspond to the reaction of the triplet state of an aromatic ketone with a hydrocarbon (Scheme VII). Infrared spectra indicate that the radicals **6e,g** contain a CO bond with large double-bond character (strong band at 1600 cm^{-1}), whereas the diamagnetic metal oxyporphyrins have a C-OH single bond. This might explain why the excited state of **6e,g** possesses a reactivity on the C=O bond in analogy to benzophenone, which is not found in the oxyporphyrins (**4e,g**). However, it must be remembered that the overall spin state of the excited state of the oxophlorine radical is a quartet and this system will have much shorter lifetimes[22] than a normal triplet of benzophenone type. The electronic spectra of oxaporphyrins and their metal compounds are similar to those of metal biliverdinates. The low numerical values of oxidation and reduction potentials and the instability of π radicals are also comparable to those of bilatrienes with an open macrocycle. The ^1H NMR, however, produce chemical shifts of the methine protons which point to a ring current comparable to the one found in porphyrins. Therefore ^1H NMR chemical shift behavior cannot be correlated with chemical behavior of these tetrapyrrolic chromophores.

Conclusion

The chemistry of oxophlorines is determined by the reactivity of their π radicals, which are easily formed under various conditions. This is somewhat comparable to the reactivity patterns of phenols.[23] Addition of oxygen at centers of high spin chemistry, opening and reclosure of the tetrapyrrolic macrocycle, and intramolecular cyclization of the "phenolic" oxygen with carbon substituents are important reactions of oxophlorine radicals. Under appropriate experimental conditions, all reactions proceeded with yields over 70%. No direct evidence for formation of σ-bonded dimers, analogous to the products from phenoxy radicals, could be produced. Oxophlorine radicals rather form diamagnetic π-π' dimers like metalloporphyrin radicals.

Although the occurrence of oxophlorines in biological systems has not been demonstrated so far, they could play a central role in many conversions concerning the porphyrin π system.[24,25] Degradation of heme to biliverdin[4] is the most obvious candidate and has been discussed in connection with Scheme VI. In the biosynthesis of protoporphyrin and chlorophyll, the oxygenation of the carbon substituents in a porphyrin precursor might proceed through oxophlorine formation, cyclization analogous to Scheme VII, and subsequent cleavage of the oxole ring. In the pathways from porphyrinogens to corrins, there is also the possibility of an oxophlorine intermediate which could undergo decarbonylation and ring contraction. We feel, that these admittedly highly speculative suggestions are in place here, because oxophlorines are so easily formed from porphyrins in vitro, and their most important reactions lead to products, which are not far from some natural products derived from porphyrins.

Experimental Section

Electronic spectral measurements and spectrophotometric titrations were performed on a Zeiss DMR 21 spectrophotometer with a variable temperature accessory. Infrared (ir) data were obtained using a Perkin-Elmer Model 521. Proton magnetic resonance (^{1}H NMR) spectra were recorded with a Varian Associates HA-100; chemical shifts are expressed in parts per million downfield from tetramethylsilane in units of δ. ESR spectra were obtained with a Bruker B-ER 414 S ESR spectrometer operating at x band with 100-kHz field modulation. The magnetic field was calibrated by the aid of an Al 675 Alpha NMR Gauss meter model and, for low temperature measurements, Bruker unit B-ST 100/700 was used. Redox potentials were determined with a Metrohm Polarecord E 261 polarograph including Model E 446 iR compensator. A three-electrode set-up was used with a saturated calomel as reference. Oxidation potentials were measured with a rotating platinum electrode in *n*-butyronitrile as solvent, and reduction potentials were obtained with a dropping mercury electrode in dimethyl sulfoxide. In some cases, the reversibility of the reactions was checked by cyclic voltammetry measurements with a stationary platinum disk electrode (Beckman Model 39273) using a McKee-Pedersen MP 1502 voltammetry module. Triangular sweeps were generated with the help of MP-1042 voltammetry controller module. The cyclic voltammograms were recorded by Siemens Model M 73924 xy recorder. Sweep rates were varied between 0.16 and 0.01 V/sec. The peak potentials measured with respect to SCE were independent of sweep rate in this range. The measurements on the Zn complex of **1a** were done in the dark to avoid decomposition. Melting points are uncorrected. Analytical thin layer chromatography (TLC) was performed on Merck 0.25-nm precoated silica gel plates; preparative TLC was conducted on 1.0-nm precoated silica gel plates. Dry columns using alumina (grade III, Woelm) or silica gel, both the absorbants being "dry-column" grade (Woelm, no indicator). *n*-Butyronitrile for voltammetry was refluxed twice over potassium permanganate and distilled. Dimethyl sulfoxide was distilled under reduced pressure shortly before use. Irradiation was performed with an air-cooled Hedler movie light, which was equipped with an Osram 1000-W halogen-tungsten bulb. Microanalyses were performed by I. Beetz, Kronach, West Germany.

Temperature-Jump Experiments. Temperature-jump experiments were carried out on an improved version of the Eigen-de Maeyer temperature-jump apparatus, the details of which have appeared elsewhere.[26,27] A 0.1 *M* solution of tetra-*n*-butylammonium perchlorate in chloroform was used as the ionic medium. It was shown by uv and ESR spectroscopy that the electrolyte did not affect the extinction coefficients or equilibrium constants. Temperature jumps were executed at various temperatures between 5 and 28°C. A discharge voltage of 14 V resulted in a rise of 2°C. Four temperature-jump measurements were performed on each sample at intervals of 5 min for temperature equilibration. The evaluation of the data followed standard procedures.

A. Dimerization of α-Oxooctaethylphlorine Radical 6a. Preliminary experiments showed that electric discharges between platinum electrodes caused rapid and irreversible reaction of the radical. Apart from the changes in the absorption spectrum occurring due to the dimerization of the radical, additional changes had appeared, indicating the formation of α,γ-porphodimethene. The latter changes could be almost completely avoided by maintaining an inert gas (N_2, Ar) atmosphere and the use of gold electrodes. Under these conditions, the relaxation effects were reproducible. The absorption changes were observed at 405 nm. The relaxation curves could be fitted within the limits of error to a single exponential with relaxation times between 3.1×10^{-3} and 1.53×10^{-3} sec, depending upon the concentration.

For a dimerization, the relaxation time is related to the rate constants k_R (recombination) and k_D (dissociation) and to the free concentration of monomers C_R on total concentration C_0, respectively

$$1/\tau = 4k_R C_R + k_D$$

or after replacing C_R by C_0, k_R, and k_D

$$1/\tau^2 = 8k_R k_D C_0 + k_D^2$$

The linear dependence of $1/\tau^2$ upon C_0 is demonstrated in Figure 7. This is a kinetic proof which is independent of equilibrium measurements that in fact a dimerization reaction has occurred. k_D and k_R can be evaluated both from the intercept and slope in Figure 7. The resulting equilibrium constant $K = k_R/k_D$ of 10^4 M^{-1} is in satisfactory agreement with the value of 5×10^3 M^{-1} taken from equilibrium measurements, if one considers that k_D is only of low accuracy. Therefore, k_D is replaced by k_R/K, where K is taken from equilibrium measurements, and a more accurate value of k_R is obtained from the slope in Figure 7. An Arrhenius plot of log k_R against $1/T$ yielded an activation enthalpy of the recombination reaction $\Delta E_R = -4(\pm 2)$ kcal/mol.

B. Dimerization of Nickel α-Oxyoctaethylporphyrin Radical 6b. The absorption changes were followed at 600 nm. At low concentration, two relaxation effects are observable, one in the time range around 500 μsec and the second faster than 200 μsec, the amplitude of which was only 20–30% of the former one. The fast effect could not be evaluated quantitatively and was not resolvable from the main effect at higher concentrations. For the main effect, the plot $1/\tau^2$ against C_0 was only linear in the range between 1.0×10^{-5} and 5.0×10^{-5} M and leveled off at higher concentrations. The concentration dependence of $1/\tau^2$ for low C_0 values shows unequivocally that also, in this case, a dimerization is observed. The fast relaxation effect as well as the saturation of $1/\tau^2$ may have the same reason that a second reaction step precedes or follows the dimerization and becomes rate determining at higher concentration. The rate constants given in Table I are evaluated only from the linear part of the plot $1/\tau^2$ against C_0. An equilibrium constant $K_{20°} = 9 \times 10^3$ M^{-1} was evaluated from these data, which agreed within the given limits of error with the constant obtained from temperature dependent ESR measurements (6×10^3 M^{-1}).

Products from the Oxidation of Zinc Octaethylporphyrin 7b with Thallium Trifluoroacetate. Zinc octaethylporphyrin (830 mg), synthesized by Professor H. Pommer, BASF, following a procedure of Inhoffen,[15] was converted into **1a** by oxidation with thallium trifluoroacetate[13] and subsequent demetallation with hydrochloric acid. The resulting mixture of octaethylporphyrin (~5%), octaethyloxophlorine **1a** (60%), α,γ-dioxooctaethylporphodimethene **8a** (5%) and α,β-dioxooctaethylporphomethene **12** (4%) was chromatographed on an alumina column (3.0 × 60 cm) with methylene

chloride. Homogeneous fractions were combined and evaporated.

α,γ-Dioxooctaethylporphodimethene (8a). This was the second fraction eluted from the chromatography of the above mixture (after octaethylporphyrin) and was crystallized from methylene chloride-methanol in the form of long, brown rectangular plates: 40 mg (5% from **7b**); mp 270-75°C; (M^+ + 2) 556 (100%), M^+ 564 (48%); NMR ($CDCl_3$) δ 6.64 (singlet, 2 methine H), 2.7, 2.48 (2 quartets, 8 CH_2), 1.12, 1.10 (2 triplets, 8 CH_3); λ_{max} ($CHCl_3$) 490 (16000), 410 (70000), 316 (33000); ir (KBr) 1602 cm^{-1} (CO).

Anal. Calcd for $C_{36}H_{44}N_4O_2$ (564.6): C, 76.6; H, 7.8; N, 9.9. Found: C, 76.7; H, 7.83; N, 9.62.

α,β-Dioxooctaethylporphomethene Hydrate (12). This was the third fraction and was also crystallized from methylene chloride-methanol: 35 mg (4% from **7b**); mp 288-291°C; (M^+ + 2) 566 (100%), M^+ 564 (60%); NMR ($CDCl_3$) δ 9.96 and 8.69 (singlets for 1 H each, exchangeable with D_2O) 6.65, 4.66 (two singlets for 1 H each), 2.0-2.9 (multiplet, 8 CH_2), 0.9-1.44 (multiplet, 8 CH_3); λ_{max} ($CHCl_3$) 537 (8200), 344 (27000); ir (KBr) 1595 cm^{-1} (CO). Addition of zinc acetate in methanol did not change the spectrum.

Anal. Calcd for $C_{36}H_{44}N_4O_2$ (**12a**) (564.6): C, 76.59; H, 7.80; N, 9.93 [for $C_{36}H_{46}N_4O_3$ **12b** (582.6): C, 74.23; H, 7.96; N, 9.61]. Found: C, 75.11; H, 8.49; N, 8.55.[28]

The actual analysis, therefore, points to about half a mole of water.

Oxooctaethylphlorine 1a. This blue fraction eluted fourth from the column and was crystallized from methylene chloride-methanol as blue needles: 412 mg (54% from **7b**); mp 255-257°C; M^+ 550 (100%); NMR ($CDCl_3$, at −30°C) δ 8.1 (singlet 2 CH), 7.6 (1 CH), 3.1-3.5 (multiplet, 8 CH_2), 1.1-1.6 (multiplet, 8 CH_3); λ_{max} ($CHCl_3$) 635 (18700), 586 (10100), 404 (170000); ir (KBr) 1570 cm^{-1}.

Anal. Calcd for $C_{36}H_{46}N_4O$ (550): C, 78.5; H, 8.42; N, 10.17. Found: C, 78.34; H, 8.42; N, 9.09.

Zinc α-Oxyoctaethylporphyrin (3c). The oxophlorine **1a** (100 mg) was dissolved in 10 ml of chloroform, and a solution of 50 mg of zinc acetate in 1 ml of methanol was added. The solution was shortly heated to 60°C in the dark and concentrated to a volume of about 3 ml, and 5 ml of hot methanol was added. Red needles (105 mg) were isolated. The compound was light sensitive in solution: no melting point below 300°C; M^+ 612 (100%), M^+ − 29 583 (−CO, 67%); λ_{max} (CH_2Cl_2) 568 (6600) 534 (12700) 406 (220000); ir (KBr) 3510 (m, OH) 1585 cm^{-1} (w, C=O).

Nickel α-Oxyoctaethylporphyrin (3b). In a 250-ml three-necked flask (N_2 inlet, reflux condenser, dropping funnel), 150 ml of acetic acid was refluxed in a nitrogen stream, and 275 mg of the oxophlorine **1a** was added. To this blue-green solution, 3 ml of a saturated nickel acetate solution in acetic acid was dropped. After 10 min of further refluxing under nitrogen, the solution turned red. The flask was then carefully sealed under nitrogen and slowly cooled to room temperature. The nickel complex crystallized as violet squares (mother liquor, green-brown) and was centrifuged: 250 mg (82%); no melting point below 300°C; M^+ 606 (100%); λ_{max} ($CHCl_3$) 556 (10300), 523 (12100), 405 (170000); ir (KBr) 3540 (s, OH) 1600 cm^{-1} (vw, C=O).

Octaethyloxophlorine Radical 6a and Its Dimer. The oxophlorine **1a** (500 mg) was chromatographed on an alumina column (3 × 60 cm) with methylene chloride for about 1 hr in the presence of air. It could then be observed on the column that the blue color of the starting material had changed to light green. When this was complete, the material was rapidly eluted from the column by raising the flow rate, the solvent was evaporated, and the residue crystallized from methylene chloride-methanol: 460 mg (90%) of green platelets; mp ~270°C dec; M^+ 550 (100%); λ_{max} (*t*-BuOH) 750 (4000), 638 (5800), 472 (7200), 411 (70000); ir (KBr) 1602 cm^{-1} (s). The susceptibility of this compound was determined by Evans' NMR shift method.[29] Measurements were done with ca. 10^{-3} *M* solutions of **6a** in $CHCl_3$ with tetramethylsilane as reference. The contact shifts of Me_4Si were of the order of 1-2 Hz. (For example, for a 0.0034 *M* solution of **6a**, the shift was 0.95 ± 0.05 Hz in a 60-MHz spectrometer. This corresponds to a magnetic susceptibility of 1.6 μ_B. Theoretical value for a spin ½ system: 1.7 μ_B.)

Anal. Calcd for $C_{36}H_4N_4O$: C, 78.69; H, 8.20; N, 10.20. Found: C, 78.40; H, 8.36; N, 9.15.

More extended exposure of **1a** to air either in solution or on alumina led to slow and almost quantitative conversion to the α,γ-dioxoporphodimethene (**8a**).

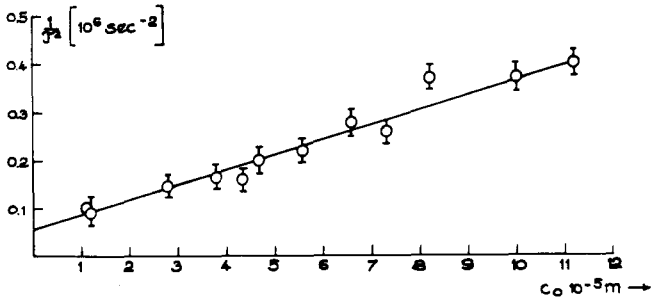

Figure 7. Plot of the inverse square of the relaxation time $1/\tau^2$ vs. the concentration of octaethyloxophlorine radical.

The solid dimer of the above radical was obtained when 3 ml of chloroform solution of 50 mg of the radical was cooled to −65°C (Dry Ice-acetone) and the solvent was slowly evaporated (ca. 24 hr) in vacuo: M^+ 1098 (25%), (M^+ − 294) 804 (100%); ir (KBr) 1602 cm^{-1} (CO, not significantly different from the monomeric radical; measurements in chloroform at different temperatures did not produce changes in the intensity of this band).

Zinc Oxyoctaethylporphyrin Radical 6c. The metal free radical **6a** (100 mg) was dissolved in chloroform and mixed with a few drops of saturated methanolic zinc acetate solution. There was an immediate color change from green to brown. More methanol was added, and brownish needles (105 mg) were centrifuged: no melting point below 300°C; M^+ 612 (100%); λ_{max} ($CDCl_3$) (broad bands) 812 (9200), 705 (3000), 480 (8200), 430 (102000); ir (KBr) (no OH) 1580 (s, C=O); ESR g = 2.0040.

Nickel Oxyoctaethylporphyrin Radical 6b. The nickel oxyporphyrin **3b** was chromatographed on silica gel with benzene-petroleum ether (40-60°C) (1:1) in the presence of air. Behind a fast running brown zone, the green fraction of the required radical was eluted. Crystallization from chloroform-methanol yielded brown rhombic crystals: 70 mg (64%); no melting point below 300°C; M^+ 606 (100%); λ_{max} ($CHCl_3$, 25°C) (broad bands) 850 (1150 from dimer), 770 (2800 from monomer), 600 (5300), 445 (54000), 407 (50000); λ_{max} ($C_6H_5CH_3$, 25°C) 770 (4300), 600 (4900), 445 (61000), 408 (50000); ir (KBr) 1620, 1597 (s, CO); NMR ($CDCl_3$, −40°C, broad signals) δ 6.61 (2 H), 6.48 (1 H), 7.7 (16 H), 9.0 (24 H); NMR ($CDCl_3$, −80°C, broad signals) δ 6.70 (2 H), 6.50 (1 H), 7.6 (16 H), 8.85 (24 H).

Anal. Calcd for $C_{36}H_{43}N_4ONi$: C, 71.28; H, 7.10; N, 9.24. Found: C, 70.20; H, 6.96; N, 9.13.

Zinc Oxaoctaethylporphyrin 9b. A. By photooxygenation of zinc oxyporphyrin **4c**, 5×10^{-5} *M* solutions of **4c** in dry benzene or benzene-methylene chloride mixture (1:1) were irradiated in glass cylinders (φ 5 cm, height 30 cm) with a 1000-W movie light from a distance of 50 cm. After 15-20 min, the 662-nm absorption band of the oxaporphyrin **9b** had reached maximum height, and the reaction was stopped. The solvent was removed and the residue chromatographed on silica gel with chloroform. Starting material and some brown decomposition products were thus eluted, and the oxaporphyrin stayed on the top of the column. It was finally removed with chloroform-methanol (92:8) and crystallized from the same solvent mixture: yields 10-15% of **9b** and 60-70% of starting material and its π radical.

B. By cyclization of zinc octaethylbiliverdin **11c**, 25 mg of **11c** was dissolved in 10 ml of chloroform, and 30 mg of zinc acetate in methanol was added (λ_{max} 690 nm). The solvent was evaporated and the residue redissolved in 10 ml of chloroform and 2 ml of acetic anhydride. This mixture was refluxed for 2 min, cooled to room temperature, washed with water, and again evaporated. The residue was chromatographed on silica gel with chloroform-methanol (92:8) and the major component crystallized from chloroform-methanol: 23 mg (84%); no melting point below 300°C; mol wt (high resolution mass spectra) (M^+ + 1) 600.2792 (calcd for $C_{35}H_{44}N_4O$ ^{64}Zn, 600.2806), 602.2763 (calcd for $C_{35}H_{44}N_4O$ ^{66}Zn, 602.2775) (The intense M^+ + 1 peak at *m/e* 600 instead of an M^+ peak at *m/e* 599 is explained by the usual hydrogenation of tetrapyrroles of low reduction potential in the mass spectrometer[33] and subsequent deprotonation); λ_{max} ($CHCl_3$) 662 (32000), 620

(sh, 6900), 550 (6000), 515 (4800), 394 (27000), 335 (17000); ir (KBr) weak bands between 1600 and 1730 cm^{-1}; NMR ($CDCl_3$) δ 9.27 (s, 1 CH), 9.18 (s, 2 CH), 3.48-3.7 (m, 16 CH_2), 1.6-1.8 (24 CH).

When a methanolic solution of **11b** was shortly shaken with solid silver(I) oxide, the same oxaporphyrin **9b** was obtained in high yield.

Anal. Calcd for $C_{35}H_{43}N_4OZnCl$ (636.4) (from procedure A): C, 66.06; H, 6.81; N, 8.80; Cl, 5.57. Found: C, 65.36; H, 7.14; N, 7.88; Cl, 4.22.

After recrystallization from a chloroform solution which had been repeatedly washed with NH_4Cl solution and drying in high vacuo at 80°C. Found: C, 66.53; H, 6.69; N, 9.23; Cl, 5.96.

Octaethylbiliverdin 11a. To a solution of 5 mg of the zinc oxaporphyrin **11c** in 5 ml of methanol, 0.5 ml of tetramethylammonium hydroxide in methanol (20%) was added. The color changed from blue-green to light green. After 1 min, 2 ml of hydrochloric acid in methanol (15%) was added (→ blue) and, after another 5 min, diluted with methylene chloride, neutralized with sodium bicarbonate in water, and washed with water. The solvent was then evaporated and the residue chromatographed on silica gel with chloroform-methanol (96:4). From chloroform-methanol blue needles, mp 248-251°C, were obtained: 4.5 mg (90%); M^+ 554 (100%); λ_{max} ($CHCl_3$) 650 (14000), 370 (49000); ir (KBr) ν 3200 cm^{-1} (s, NH), 1680 (s, CO); NMR ($CDCl_3$) δ 5.88 (s, 3 CH) 2.50, 2.27 (1 q, 16 CH_2), 1.24, 1.20, 1.16, 1.08 (4t, 24 CH_3). The compound had been obtained earlier by Nolte[30] by a different pathway and was identical to our sample.

Nickel 2′,α-Oxoleoctaethylporphyrin (10a). A. From Nickel α-Oxyoctaethylporphyrin π Radical (6b). 6b (60 mg) in 1.2 l. of benzene were irradiated in three glass cylinders (diameter 4 cm) from a distance of 30 cm for 90 min under nitrogen gas. The color changed from a brownish green to red. The solvent was then removed and the residue chromatographed on silica gel with benzene-petroleum ether (1:1). The red compound which eluted first was crystallized from chloroform-methanol: 40 mg (65%); mp 264-267°C; M^+ (high resolution mass spec) 604.2705 (calcd for $C_{36}H_{42}N_4O$ ^{58}Ni, 604.2712), 606.2670 (calcd for $C_{36}H_{42}N_4O$ ^{60}Ni 606.2666); λ_{max} ($CDCl_3$) 555 (9700), 517 (8500), 480 (sh, 2700), 403 (133000); ir (KBr) (no CO or OH); NMR ($CDCl_3$) δ 9.55, 9.52, 9.43 (3s, CH), 6.56 (q, CH), 3.92 (q, 2 CH_2), 3.84 (q, 12 CH_2), 2.18 (d, 3 CH_3), 1.68-1.9 (m, 21 CH_3). The compound proved to be rather unstable, and only a few milligrams of semicrystalline material could be isolated in solid form. Therefore combustion analysis was not satisfactorily.

Anal. Calcd for $C_{36}H_{42}N_4ONi$: C, 71.42; N, 6.99; N, 9.25. Found: C, 72.68; H, 7.44; N, 9.28.

B. From Nickel Oxyoctaethylporphyrin 4b. 4b was irradiated under the same conditions as the radical 6b but in the presence of air. First the π radical **6b** was formed, which was further converted into the oxole **10a**. The yield was, however, lower than that obtained by procedure A (~10%).

Zinc 2′,α-Oxoleoctaethylporphyrin (10c) and Metal Free 2′,α-Oxoleoctaethylporphyrin (10a). Zinc oxyporphyrin radical **6c** (30 mg) in 1 l. of benzene was irradiated in a 2-l. glass flask under nitrogen with magnetic stirring for 2 hr. The solvent was then removed and the residue chromatographed on silica gel with benzene. From chloroform-methanol, 24 mg (80%) of red needles was obtained: no melting point below 300°C; M^+ 610 (100%); λ_{max} ($CHCl_3$) 569 (8300), 537 (10900), 500 (sh, 4700), 412 (270000); ir (KBr) no CO or OH bands. The complex proved to be rather unstable in solution, and no resolved NMR spectrum could be obtained.

For demetallation to **6a**, a chloroform solution of 20 mg of **6c** was washed twice with 5% hydrochloric acid, sodium bicarbonate, and water and evaporated to dryness. The residue was chromatographed as described above: yield 16 mg (80%); no melting point below 300°C; ir (KBr) no CO or OH bands; λ_{max} ($CHCl_3$) 627 (9100), 573 (4800), 546 (5800), 508 (13000), 409 (300000).

Zinc α,γ-Dioxooctaethylporphomethene (8b) (A, B). Zinc oxyporphyrin **4c** (100 mg) in 1.2 l. of dry pyridine was placed in glass cylinders (diameter 4 cm) and irradiated from a distance of 30 cm. Within a few seconds, the solution turned green and the radical **6c** appeared. After 10 min, when the solution had again changed to a red color, irradiation was stopped and the solvent removed. The residue was chromatographed on silica gel. Two main fractions were observed: a fast broad red one **8b**,A and a slower sharp one **8b**,B. Both fractions were evaporated to dryness, and the residue was recrystallized from chloroform-methanol [red product, **8b**,A, 55 mg (56%); green product, **8b**,B, 25 mg (25%)]: (both products) no melting point below 300°C; M^+ (high resolution mass spectra) **8b**,A 626.2609, **8b**,B 626.2584 (calcd for $C_{36}H_{42}N_4O_2$ ^{64}Zn; 626.2599), **8b**,A 628.2568, **8b**,B 628.2561 (calcd for $C_{36}H_{42}N_4O_2$ ^{66}Zn, 628.2568); λ_{max} ($CHCl_3$) (both products) 576 (33000), 440 (78000); ν_{max} (KBr) (red product) 580, 460; ν_{max} (KBr) (green product) 620, 580, 480; ir (KBr, both products) 1590 (s) and 1632 (m); NMR ($CDCl_3$, red product) δ 6.47 (s, 2 CH), 2.56, 2.36 (2q, 16 CH_2), 1.03, 0.98 (2t, 24 CH_3); NMR (green product) no sharp signals. Both products were dried at 80°C in high vacuo for analysis.

Anal. Calcd for $C_{36}H_{42}N_4O_2Zn$ (627.4): C, 68.86; H, 6.70; N, 8.93. Found: **8b**,B, C, 68.76, H, 6.88, N, 8.60; **8b**,A, C, 68.89; H, 7.03; N, 9.28.

Reduction of the green product with sodium dithionite in hexamethylphosphortriamide (HMPA) yielded a stable green radical (ESR g = 2.003, line width 2 G), whereas the red product decomposed rapidly and gave only a weak ESR signal.

Nickel α-Oxy-γ-formyloctaethylporphyrin (13a). The procedure was identical with the one used in ref 15 for the formylation of copper octaethylporphyrin. The main green fraction (R_f 0.5) on the silica gel column (solvent, CH_2Cl_2) used for separation of products contained **13a**, whereas a minor light green band (R_f 0.35) is presumably the β,γ-diformyl product, not described in the general text. Both products were crystallized from chloroform-methanol. A few drops of water were added: 155 mg (of **13a**) (74%); mp 269-274°C; M^+ 634 (20%), (M^+ − 28) 606 (100%); λ_{max} ($CHCl_3$) 622 (5600), 570 (sh, 400), 466 (19600), 332 (7400); ir (KBr) 1590 (s, CO), 1715 (m, CHO); no sharp NMR signals (containing free radical).

Anal. Calcd for $C_{38}H_{43}N_4O_3Ni$ (634.7): C, 70.03; H, 6.78; N, 8.83. Found: C, 70.71; H, 7.08; N, 10.46.

To the product corresponding to the second, light green fraction, tentatively the structure of the diacetal of nickel α-oxy-β,γ-diformyloctaethylporphyrin is assigned: $C_{38}H_{43}N_4O_3Ni{\cdot}2H_2O$ (661.7 + 36) (M^+ − 2) 659 (100%); λ_{max} ($CHCl_3$) 783 (20000), 400 (38000); NMR ($CDCl_3$) δ 7.72, 7.47, 7.1 (3s, 3 CH), 2.6-3.2 (m, 16 CH_2), 0.3-1.4 (m, 24 CH_3).

Oxime of 13a. 13a (50 mg), 1 g of hydroxylamine hydrochloride in 100 ml of pyridine, and 25 ml of water were refluxed for 5 hr and left overnight at room temperature. 300 ml of methylene chloride were added, washed with water, and evaporated to dryness. The residue was chromatographed on silica gal with methylene chloride. The main fraction (R_f 0.2) was collected and crystallized from methylene chloride-methanol: 46 mg (88%) of $C_{37}H_{45}N_5O_2Ni$ (649.7); no melting point below 300°C; no M^+ peak (M − 18)$^+$ 631 (−H_2O, 32%) (M − 43)$^+$ 606 (−$CNOH_2$, 100%); λ_{max} ($CHCl_3$) 563 (8000), 534 (12000), 415 (166000); ir (KBr) ν 1700 (m, C=N).

Nickel α-Acetoxy-γ-cyanooctaethylporphyrin (13c). The oxime from **13a** (40 mg) was heated to 60°C in acetic anhydride for 30 min. The mixture was then treated with 50 ml of chloroform at room temperature, washed ten times with water, and evaporated to dryness. Crystallization from methylene chloride-petroleum ether (60-80°) yielded 11 mg (26%) of large prisms of the acetoxy derivative **13c**: mp 252-256°C; M^+ 673 (54%), (M − 55)$^+$ 618 (−$OCOCH_3$ + 4H, 100%); λ_{max} ($CDCl_3$) 595 (12700), 550 (6800), 414 (114000); ir (KBr) 1765 (CO), 2205 (CN); NMR ($CDCl_3$) δ 9.32 (s, 2 CH), 4.12, 3.83, 3.85 (3q, 16 CH_2), 2.60, 1.78, 1.71, 1.69 (4t, 24 CH_3).

Anal. Calcd for $C_{39}H_{45}N_5O_2Ni$ (673.7): C, 69.50; H, 6.68; N, 10.39; Found: C, 70.04; H, 6.84; N, 9.91.

α-Mercaptooctaethylporphyrin (7e) and Its Zinc Complex 7f. This compound was prepared following a procedure by Clezy.[31] Our analytical data, however, differ somewhat from the ones reported and are therefore given: $C_{36}H_{46}N_4S$ (566.6) (M − 4)$^+$ 562 (−4H (?), 25%), (M − 32)$^+$ 534 (−S, 100%), (M − 47)$^+$ 519 (−CSH, −3H (?), 57%)[33]; λ_{max} ($CHCl_3$) 635 (5700), 620 (sh, 3600), 575 (sh, 6200), 564 (sh, 7000), 550 (8200), 535 (sh, 6900), 507 (9100), 402 (140000); ir (KBr) 2145 (s, SH); NMR ($CDCl_3$) δ 10.09 (s, 3 CH), 9.90 (s, 1 CH), 4.1 (q, 16 CH_2), 1.94, 1.85 (2t, 24 CH_3).

Anal. Calcd for $C_{36}H_{46}N_4S$ (566.7): C, 76.30; H, 8.12; N, 9.93.

Found: C, 75.77; H, 7.54; N, 10.78.

The zinc complex **7f** was prepared in chloroform by the addition of methanolic zinc acetate solution and crystallization from chloroform-methanol: $C_{36}H_{44}N_4SZn$ (630.1) M^+ 631 (25%), $(M - 35)^+$ 596 (−SH, −2 H, 100%); intense peak for dimer at 1192; ir (KBr) 2138 (SH); λ_{max} ($CHCl_2$) 595 (13500), 552 (8700), 415 (170000); NMR ($CDCl_3$) δ 9.80 (s, 3 CH), 9.18 (s, 1 CH), 4.38, 4.06, 3.62 (16 CH_2), 2.02-1.58 (m, 24 CH_3). Both mass and NMR spectra point to dimer formation of this zinc complex, presumably over a disulfide bridge. Addition of a few drops of pyridine to the chloroform solution changes to ^1H NMR spectrum and possibly breaks up the dimer: NMR δ 10.30 (s, 1 CH), 10.22 (s, 2 CH).

Reduction of α,β-Dioxoporphodimethene Monohydrate 12a to α-Oxooctaethylphlorine (1a). 12a (10 mg) was dissolved in 30 ml of methanol, and 200 mg of sodium borohydride was added. The solution decolorized slowly and, after 45 min, 1 ml of acetic acid was added. The solution turned greenish blue, was diluted with 30 ml of water, and extracted with chloroform. Evaporation of the solvent, thin layer chromatography on silica gel, and crystallization from chloroform-methanol yielded 6 mg of **1a**; which was identical in all respects (TLC, uv, ir) with authentic material.

Analysis of Carbon Monoxide in the Photooxygenation of Zinc Oxyporphyrin Radical 6c to Zinc Oxaporphyrin 9b. A. Standardization of Dräger Tubes. Decarbonylation of 10 mg of oxyporphyrin would roughly yield 0.3 ml of carbon monoxide. This amount of porphyrin could be dissolved and photooxygenized in about 200 ml of benzene. Therefore our equilibration procedure was applied in this range; a gas tube of 0.48 cm diameter and a volume of 1.60 ml, which ended in two stopcocks with a bore of 1.5 mm, was connected to a carbon monoxide tank. When carbon monoxide had replaced all of the air in the tube, the stopcocks were closed and one of them was connected to the stem of a 500-ml separating funnel and the other to a 1-l. wash bottle with a fritted disk at the end of the tubing. Both the funnel and the bottle contained 400 ml of dry benzene each. Now the three stopcocks of the funnel and the gas trap were slowly opened. The gas did not escape in bubbles but was rapidly dissolved by the benzene which ran through the trap. At the end, 800 ml of benzene, which had dissolved 1.60 ml, had been collected in the wash bottle. The small gas volume above the solution did not contain measurable quantitatives of carbon monoxide.

This solution (200 ml) containing 0.4 ml of CO was carefully transferred into another 500-ml wash bottle with a fritted disk at the end of the air inlet. The outlet was connected with a second wash bottle, which was empty and cooled with an acetone-Dry Ice mixture to freeze out solvent vapors. Its gas outlet was connected with a "Vorsatzröhrchen" (Ch 24101), which absorbed the last traces of solvents, but could also be omitted, and a Dräger-carbon monoxide tube (25601) which was fixed on a Dräger-Gasspürpumpe (100 ml; Mod. 31 CH 6709). The Dräger bellows were then pressed 15 times, which sucked 1.5 l. of air through the system, and the length of the colorization in the tube (from the formation of iodine $5CO + I_2O_5 \rightarrow I_2 + 5CO_2$) was noted. Carbon dioxide and formaldehyde did not give any coloration under identical conditions. Larger air volumes did not produce longer colorized zones in the tubes; therefore, the carbon monoxide had been quantitatively driven out of the benzene phase by this procedure. Dilutions of the standard carbon monoxide solutions and application of the same procedure yielded the other points of the standardization curve in Figure 8. Earlier experiments had been performed by slowly sucking 2 l. of pure nitrogen from a reservoir through the solution instead of air with the standard bellows, but this is a more complicated procedure and did not yield better results. A blind probe without CO in the benzene did not give any coloration of the tubes. Figure 8 shows that the length of colorization and the amount of CO dissolved in benzene depend linearly on each other. All the standards could be reproduced with high accuracy.

B. Evaluation of the Gas Evolved in the Photooxygenation. Zinc oxyporphyrin radical **6c** (6.0-9.0 mg) was dissolved in 200 ml of benzene and transferred into a 500-ml wash bottle which was closed by two stopcocks. The solution was magnetically stirred, cooled by tap water flowing over some of the bottle surface, and irradiated for 90 min from a distance of 30 cm. The wash bottle was then connected to the bellows and the Dräger tubes as described above, and 1.5 l. of air was pressed through the solution. The results are summarized in Figure 8.

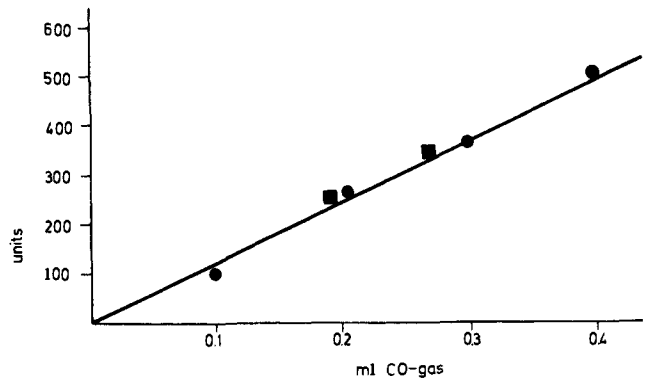

Figure 8. Plot of CO gas concentration (milliliters of CO per 200 ml of benzene) (●) from standardization with solution of known CO concentration in benzene (■) (experimental values from irradiation of **6c**).

No traces of carbon dioxide or formaldehyde using the appropriate Dräger tubes could be detected under these conditions. We believe that the carbon monoxide estimations are correct with no larger error than 3%, and that a least five times less carbon monoxide could be detected with a comparable error. Irradiation of the oxaporphyrin **9b** under identical conditions did not yield measurable quantities of CO.

Acknowledgments. This work was supported by the Bundesministerium für Forschung und Technologie, the Deutsche Forschungsgemeinschaft, and the Fonds der Chemischen Industrie. We also thank Professors H. Pommer and H. H. Inhoffen for a generous gift of octaethylporphyrin and Dr. L. Grotjahn for measurements of mass spectra.

References and Notes

(1) Preliminary reports of some of this work have been published: (a) J.-H. Fuhrhop, S. Besecke, and J. Subramanian, *J. Chem. Soc., Chem. Commun.*, 1 (1973); (b) S. Besecke and J.-H. Fuhrhop, *Angew. Chem., Int. Ed. Engl.*, **13**, 150 (1974).
(2) (a) Gesellschaft für Molekularbiologische Forschung; (b) Medizinische Hochschule, Hannover.
(3) A. H. Jackson, G. W. Kenner, and K. M. Smith, *J. Chem. Soc. C*, 302 (1968).
(4) (a) R. Tenhunen, H. Marver, N. R. Pimstone, W. F. Trager, D. Y. Cooper, and R. Schmid, *Biochemistry*, **11**, 1716 (1972); (b) T. Kondo, D. C. Nicholson, A. H. Jackson, and G. W. Kenner, *Biochem. J.*, **121**, 601 (1971).
(5) E. Stier, *Hoppe-Seyler's Z. Physiol. Chem.*, **272**, 239 (1941); **273**, 47 (1941).
(6) H. H. Inhoffen, J.-H. Fuhrhop, and F. v. d. Haar, *Justus Liebigs Ann. Chem.*, **700**, 92 (1966).
(7) R. Bonnett and M. J. Dimsdale, *J. Chem. Soc. Perkin Trans. 1*, 2540 (1972).
(8) P. S. Clezy and A. W. Nichol, *Aust. J. Chem.*, **18**, 1835 (1965); **19**, 1481 (1966).
(9) R. Bonnett, M. J. Dimsdale, and K. D. Sales, *Chem. Commun.*, 962 (1970).
(10) P. S. Clezy, A. J. Liepa, and G. A. Smythe, *Aust. J. Chem.*, **23**, 603 (1970).
(11) J.-H. Fuhrhop, P. K. W. Wasser, D. Riesner, and D. Mauzerall, *J. Am. Chem. Soc.*, **94**, 7996 (1972).
(12) P. K. Wasser and J.-H. Fuhrhop, *Ann. N.Y. Acad. Sci.*, **206**, 533 (1973); J.-H. Fuhrhop, A. Salek, J. Subramanian, Chr. Mengersen, and S. Besecke, *Justus Liebigs Ann. Chem.*, **1975**, 1131 (1975).
(13) G. H. Barnett, M. F. Hudson, S. W. McCombie, and K. M. Smith, *J. Chem. Soc., Perkin Trans. 1*, 691 (1973).
(14) J.-H. Fuhrhop, *Chem. Commun.*, 781 (1970).
(15) H. H. Inhoffen, J.-H. Fuhrhop, H. Voigt, and H. Brockmann, Jr., *Justus Liebigs Ann. Chem.*, **695**, 133 (1966).
(16) R. Pariser and R. G. Parr, *J. Chem. Phys.*, **21**, 446, 767 (1953).
(17) J. E. Bloor and B. R. Gilson, "Quantum Chemistry Program Exchange Catalog", Vol. X, 1974, Program 71.2.
(18) A. D. McLachlan, *Mol. Phys.*, **2**, 233 (1960).
(19) R. B. Woodward, *Ind. Chim. Belge*, 1293 (1962).
(20) I. V. Knop and J.-H. Fuhrhop, *Z. Naturforsch. B*, **25**, 729 (1970).
(21) J.-H. Fuhrhop, P. K. W. Wasser, J. Subramanian, and U. Schrader, *Justus Liebigs Ann. Chem.*, **1974**, 1450 (1974).
(22) R. L. Ake and M. Gouterman, *Theor. Chim. Acta*, **15**, 20 (1969).
(23) K. Dimroth, *Angew. Chem.*, **72**, 331 (1960); see also in W. Foerst, Ed., "Neuere Methoden der präparativen organischen Chemie", Vol. III, Verlag Chemie, Weinheim/Bergstr., Germany, 1961, for an extended version of this review.
(24) D. Mauzerall, *J. Am. Chem. Soc.*, **82**, 2605 (1960).
(25) J.-H. Fuhrhop, *Angew. Chem., Int. Ed. Engl.*, **13**, 321 (1974).
(26) M. Eigen and L. de Maeyer in *Tech. Org. Chem.*, **3**, 895 (1963).

(27) D. Riesner, R. Römer, and G. Maas, *Eur. J. Biochem.*, **15**, 85 (1970).
(28) Dr. K. Smith, University of Liverpool, kindly communicated to us that he found a similar product in the Tl(III) oxidation of etioiporphyrin I. The ^{1}H NMR spectrum was very similar to the spectrum reported here (two methine proton signals), and elemental analysis also yielded additional hydrogen and oxygen.
(29) D. F. Evans, *J. Chem. Soc.*, 2003 (1959).
(30) W. Noite, Dissertation, Braunschweig, 1967.
(31) P. S. Clezy and C. J. R. Fookes, *Chem. Commun.*, 1268 (1971).
(32) The X-ray analysis of crystalline green material **8b,B** revealed that this material contains a molecule of methanol as fifth ligand on each zinc ion. This did not show up in the elemental analysis; it may have evaporated on drying in high vacuum. The methanolic proton is hydrogen bonded to a ketone oxygen of a neighboring dioxoporphomethene molecule. Therefore two methanol molecules connect two chromophore molecules. The facile reducibility of this system, if it also occurred in solution, could be explained by the possibility of a proton shift toward the primarily formed anion radical to form a semiquinone-type of radical. The crystals for the X-ray analysis were obtained by crystallization from chloroform–methanol and recrystallization from ethanol. The crystal solvent molecule was exclusively methanol. Therefore the assumption of stability of this dimer in solution seems justified. The X-ray analysis of the red compound **8b,A** is in progress. We predict it to be the nonhydrogen bonded monomer of α,γ-dioxoporphodimethene (**8b**). We thank Dr. W. S. Sheldrick for allowing us to publish this note before publication of his structural work.
(33) H. Budzikiewicz and S. E. Drewes, *Justus Liebigs Ann. Chem.*, **716**, 222 (1968).

Methods in Alkaloid Synthesis. Imino Ethers as Donors in the Michael Reaction

Barry M. Trost*[1] and Robert A. Kunz

Contribution from the Department of Chemistry, University of Wisconsin, Madison, Wisconsin 53706. *Received April 14, 1975*

Abstract: Iminoethers serve as Michael donors toward α,β-unsaturated ketones provided the initial adduct is rapidly trapped. Ketal formation via amide acetals as the ketalizing agent constitutes a novel trapping method. Alternatively, rapid prototropic shift followed by cyclization onto the imino carbon when utilizing methyl 3-oxo-4-pentenoate also succeeds. The latter offers a convenient approach to 3,4,6,7,8,9-hexahydro-2-quinolizones, a good building block in alkaloid synthesis. The direct C-alkylation of lactims even with moderately unreactive alkyl halides and the synthesis of 2-cyanomethyldithiane and 5,5-trimethylenedithio-3-oxo-1-pentene, potentially useful reagents, are described.

The Michael reaction is an important synthetic method for creation of a wide range of structural types. For example, it serves as the key step in the Robinson annelation sequence. While many nucleophiles, including enolates of carbonyl systems, amines, thiols, etc., have served as Michael donors, secondary amides do not generally serve in this capacity, presumably because of an unfavorable equilibrium. In conjunction with an interest in the total synthesis of alkaloids, we became intrigued with the use of lactims, e.g., **1**, as Michael donors. Such a reaction could provide a facile entry into quinolizidines which form an important part of many alkaloids, e.g., lycopodine, yohimbine, lupinine, sparteine, eburnamine, etc. In particular, the 3,4,6,7,8,9-hexahydro-2-quinolizone (**2**) is an attractive building block,

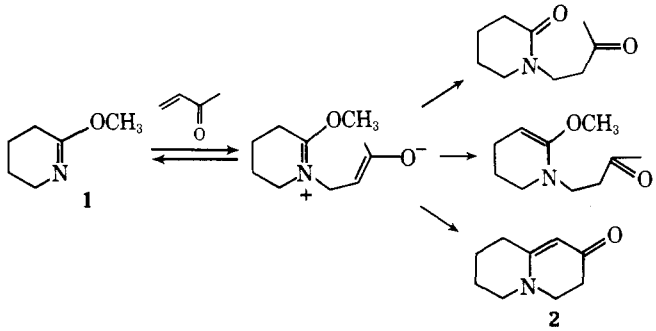

however, not readily accessible.[2,3] Its formation via a Michael reaction is complicated by the anticipated enhanced reversibility of formation of the initial adduct because of the excellent leaving-group abilities of the imino ether. Indeed, attempts to condense 2-methoxy-3,4,5,6-tetrahydropyridine (**1**) with methyl vinyl ketone lead to no reaction. In this paper, we report the realization of this approach by trapping the initial Michael adduct in an irreversible fashion and its application for the synthesis of the hexahydro-2-quinolizones.

Preparation of Starting Materials. The systems chosen for study were the parent lactim **1** and the 3-alkylated lactims **3**. The lactims **3** were prepared by the alkylation of the lithium derivative of **1** with 1-iodo-3,3-ethylenedioxybutane and 1-iodo-3-methyl-3-butene, respectively.[4,5] The latter was available from isobutylene by the method outlined in eq 1.[6] Generation of the anions required the use of nonnucleo-

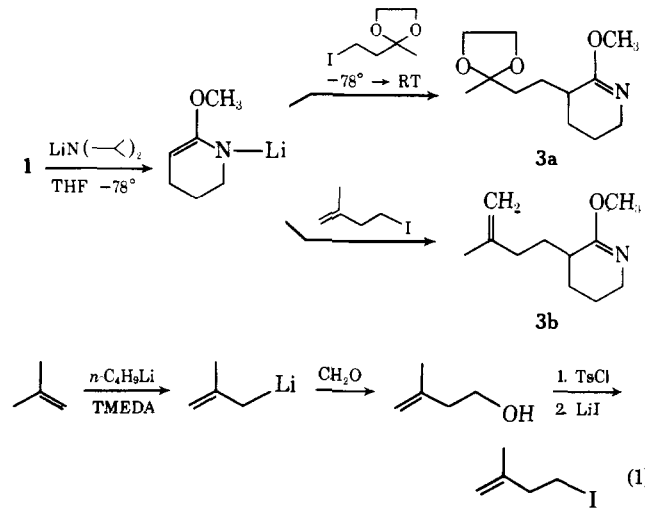

(1)

philic bases like lithium diisopropylamide. Carbon–carbon bond formation proceeded smoothly with no complications of N-alkylation. Since the imino ethers can be hydrolyzed to the lactams, this represents a useful approach for C-alkylation of secondary amides (lactams).

The initial Michael acceptor examined was dithiane **4b**.